Tunneling Ionization of Autolocalized DX^- Centers in Terahertz Fields

S. D. Ganichev,* I. N. Yassievich,* and W. Prettl
Institut für Experimentelle und Angewandte Physik, Universität Regensburg, D 93040 Regensburg, Germany

J. Diener and B. K. Meyer
Technische Universität München, Physik Department E16, D 85747 Garching, Germany

K. W. Benz
Kristallographisches Institut, Universität Freiburg, D 79104 Freiburg, Germany
(Received 27 December 1994)

Tunneling ionization of DX^- centers in $Al_xGa_{1-x}Sb$ has been observed in terahertz radiation fields. Tunneling times have been measured for autolocalized and on-site deep impurities. It is shown that in one case the tunneling time is smaller and in the other larger than the reciprocal temperature multiplied by a universal constant due to the different tunneling trajectories. This allows one to distinguish in a direct way between the two types of configuration potentials of impurities.

PACS numbers: 71.55.–i, 72.20.Ht, 72.40.+w

Defect engineering of material properties is one of the key issues of present semiconductor technology. Two remarkable examples of high current interest are the *EL2* defect in GaAs [1] and the *DX* center in III-V ternary alloys like AlGaAs, AlGaSb, etc. [2–4]. The *EL2* center is a growth defect that is responsible for the semi-insulating properties of GaAs, whereas *DX* centers are dopant-induced defects. These defects have been studied extensively in the past, stimulated by the phenomenon of metastability that both defects have in common. Here we will deal with the *DX* center. Shallow *n* dopants in ternary III-V alloys coexist in two charged states as ionized effective-mass-like donors and as deep negatively charged DX^- centers. By light illumination the DX^- center can be made electrically and optically inactive. The large difference between optical ε_o and thermal ε_T activation energies and the presence of persistent photoconductivity observed for these centers has been explained by a model of large lattice relaxation leading to autolocalization [5,6].

Figure 1 presents two adiabatic potential diagrams with a shift in the configuration coordinate of the equilibrium position, which correspond to electron-phonon coupling with [Fig. 1(a)] and without [Fig. 1(b)] autolocalization. The configuration of Fig. 1(a) is usually assumed to apply to DX^- centers, giving a big difference between ε_o and ε_T [2–6]. The configuration of Fig. 1(b) corresponds to on-site impurities. In this case the difference between ε_o and ε_T is usually small but can also be very large as shown by Henry and Lang [7] for "state 2" oxygen in GaP. The large difference has been introduced by taking two different vibrational frequencies for the occupied state and the unoccupied state, respectively. The details of the adiabatic potential configuration are of great importance for the nonradiative capture of free carriers. Extremely small capture cross section may result from autolocalization but also from lack of intersection of the bound state and the conduction band as observed in GaP [7].

Here we demonstrate that tunnel ionization in terahertz fields [8–10] allows in a simple way a clear-cut distinction between the two types of potential configurations shown in Fig. 1. The tunneling time, caused by the rearrangement of the lattice during detachment of the electron, is systematically different for both situations. To be more precise, the tunneling time is in one case smaller, in the other bigger, than the reciprocal temperature multiplied by a universal constant.

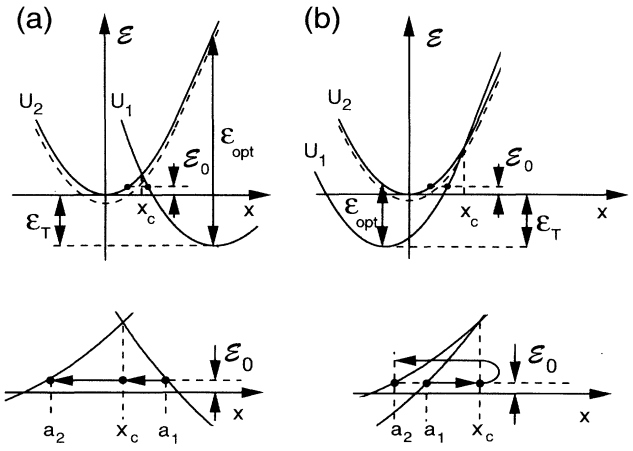

FIG. 1. Upper plates: Adiabatic potentials as a function of the configuration coordinate x of impurity motion for two possible schemes (a) with and (b) without autolocalization. ε_T and ε_{opt} are thermal and optical activation energies, respectively. Solid curves U_1 and U_2 correspond to the carrier bound to the center and detached from the impurity at the bottom of the band ($\varepsilon = 0$), respectively. The dashed curves are the potentials of an ionized impurity in an electric field. Bottom plates: Blown up representations of the tunneling trajectories.

 0031-9007/95/75(8)/1590(4)$06.00 © 1995 The American Physical Society

Measurements have been carried out on DX^- centers in $Al_xGa_{1-x}Sb$. The results will be compared to the on-site impurity gold in germanium. Large electric field strengths have been applied by high-power terahertz radiation. It has been shown previously that the electric field of terahertz radiation acts like a dc field as long as the radiation frequency is smaller than the vibration frequency of the deep impurities [10].

Multiphonon tunnel ionization in strong electric fields has been investigated for various impurities [8,10]. In Fig. 1 the curves U_1 and U_2 correspond to the ground state and to the ionized center with zero kinetic energy of the charge carrier, respectively. The impurities can be ionized by thermal excitation in the potential U_1 to an energy above the minimum of the ionized configuration U_2 and by tunneling from the bound configuration U_1 to U_2 [8,9]. In thermal equilibrium the multiphonon tunnel ionization rate is balanced by the capture of free carriers. In the presence of an electric field E the potential U_2 is shifted to lower energies as a whole (dashed curves in Fig. 1), yielding in semiclassical approximation an excess emission rate [8]

$$e(E) \propto \exp\left(\frac{(eE)^2\tau_2^3}{3m^*\hbar}\right), \tag{1}$$

where m^* is the effective mass of free carriers and

$$\tau_2 = \sqrt{\frac{M}{2}} \left| \int_{a_2}^{x_c} \frac{dx}{\sqrt{U_2(x) - \mathcal{E}_0}} \right| \tag{2}$$

is the tunneling time [11] along the trajectory from a_2 to x_c (see Fig. 1) in the configuration space under the potential U_2 at the energy $\mathcal{E} = \mathcal{E}_0$.

In this relation M is the mass of the defect and $\mathcal{E}_0$ is the optimum energy of tunneling [8,9]. The energy $\mathcal{E}_0$ decreases with decreasing temperature and approaches the minimum of the potential U_2 in the limit $T \to 0$. Thus τ_2 is strongly temperature dependent, diverging for $T \to 0$.

The temperature dependence of τ_2 may be determined from the condition of optimum tunneling. As long as the electric field is not too high to change $\mathcal{E}_0$ significantly, τ_2 may be calculated in thermal equilibrium ignoring the electric field. In this case and in the semiclassical approximation the thermal emission rate is given by $P(\mathcal{E}) \propto \exp(-\psi)$ with $\psi(\mathcal{E}) = (\varepsilon_T + \mathcal{E})/k_BT + 2|S(\mathcal{E})|$, where $S(\mathcal{E})$ is the principal function multiplied by $i/\hbar$ after [8]. Because of the exponential dependence of $P(\mathcal{E})$ on the energy $\mathcal{E}$, tunneling takes place at energies in a narrow range around $\mathcal{E} = \mathcal{E}_0$ where $\psi(\mathcal{E})$ assumes a minimum, i.e., $d\psi/d\mathcal{E} = 0$. After [8,12] $S(\mathcal{E})$ is to be split into two parts, $S(\mathcal{E}) = -S_1(\mathcal{E}) + S_2(\mathcal{E})$, with

$$S_i(\mathcal{E}) = \frac{\sqrt{2M}}{\hbar} \int_{a_i}^{x_c} dx\sqrt{U_i(x) - \mathcal{E}}\,, \qquad i = 1,2\,. \tag{3}$$

This corresponds to tunneling from a_1 to x_c under the potential U_1 and from x_c to a_2 under potential U_2. These tunneling trajectories are indicated by arrows on Fig. 1. The condition for finding $\mathcal{E}_0$ is given by

$$\left.\frac{d\psi}{d\mathcal{E}}\right|_{\mathcal{E}=\mathcal{E}_0} = 2\left.\frac{d|S(\mathcal{E})|}{d\mathcal{E}}\right|_{\mathcal{E}=\mathcal{E}_0} + \frac{1}{k_BT} = 0\,. \tag{4}$$

The essential difference between the two models discussed here is that $S_1(\mathcal{E})$ and $S_2(\mathcal{E})$ have the same signs for the on-site configuration [Fig. 1(b)] but the signs are opposite for autolocalization [Fig. 1(a)]. Thus we have $|S| = |S_1| + |S_2|$ for autolocalization and $|S| = |S_1| - |S_2|$ for the on-site configuration, taking into account that $|S_2| > |S_1|$ (see Fig. 1). The magnitude of the derivative $|dS_i/d\mathcal{E}|$ yields the tunneling times τ_1 and τ_2 along trajectories under the corresponding potentials:

$$\tau_i = \hbar \left| \left.\frac{dS_i}{d\mathcal{E}}\right|_{\mathcal{E}=\mathcal{E}_0} \right|, \qquad i = 1,2\,. \tag{5}$$

From Eqs. (4) and (5) we find

$$\tau_2 = \frac{\hbar}{2k_BT} \pm \tau_1\,, \tag{6}$$

where the minus and plus signs correspond to Figs. 1(a) and 1(b), respectively. As $\mathcal{E}_0$ is much larger than the minimum of U_1, τ_1 is approximately the period of oscillations in U_1 and does not significantly depend on temperature and electric field. For on-site deep impurities like Au, Hg, Zn, and Cu in germanium it has been shown that τ_2 is larger than $\hbar/2k_BT$ and follows the temperature dependence of Eq. (6) [8,10]. For autolocalized states τ_2 is expected to be smaller than $\hbar/2k_BT$.

The investigations of phonon-assisted tunneling have been carried out on $Al_xGa_{1-x}Sb$ samples grown by the traveling heater method from Sb-rich melts. Tellurium was added into the melt resulting in n-type conduction ($n = 4 \times 10^{17}$ cm^{-3}). The crystals were characterized by the Hall effect, deep level transient spectroscopy (DLTS), and photocapacitance measurements. All the essential features of the DX^- centers, in particular, persistent photoconductivity, have been observed. The actual sample compositions were $x = 0.28$ and 0.5. More details of the properties of the samples can be found elsewhere [13–15].

The radiation source used was a pulsed far-infrared molecular laser optically pumped by a TEA CO_2 laser. Using NH_3 and D_2O as active gases, 40 ns pulses with a peak power of 100 kW have been obtained at wavelengths λ of 90.5, 152, and 250 μm. The corresponding photon energies of 13.7, 8.2, and 5 meV, respectively, are much smaller than the ionization energies of the DX^- centers. The radiation was linearly polarized. The $Al_xGa_{1-x}Sb$ samples were placed in a temperature variable optical cryostat. Measurements have been carried out in the temperature range between 40 and 90 K where the impurity centers are occupied in thermal equilibrium. A series of cold and warm black polyethylene (1 mm thick), Teflon, and crystal quartz windows was used to transmit

far-infrared radiation while rejecting near-infrared and visible light. A photoconductive response was found at all three wavelengths. Signals were measured using a standard 50 Ω load resistor circuit, taking care that the bias voltage across the sample was substantially below the threshold of electric impurity breakdown.

The signals consist of two components (see inset of Fig. 2), a fast component with decay time of about 80 ns and a long tail, which did not decay within the presented time scale of Fig. 2. Measurements of the radiation-induced conductivity change of the sample by a dc voltmeter have shown that this part of the signal persists for several hundreds of seconds, which corresponds to the lifetime of persistent photoconductivity observed for DX^- centers in investigated samples [15]. The sign of the photoconductive signal indicates a decrease in the sample resistance and, thus, an increase in the free carrier concentration.

The observation of a positive persistent photoconductivity shows that this signal is caused by the detachment of electrons from DX^- centers. The fast component of the signal can be attributed to ionization of native Ga acceptors [16] or μ photoconductivity due to electron heating and is not of interest for the present work. Because of the large difference in relaxation time, the signals may easily be distinguished and investigated at the same time. All data will be further related just to the slow component of the signal. Figure 2 shows the dependence of $\ln(\sigma_i/\sigma_d)$ on the square of the amplitude of the optical electric field for two different wavelengths and temperatures, where σ_d and σ_i are the dark and irradiation-induced conductivities of the sample, respectively. As the duration of the light pulses is much shorter than the capture time of nonequilibrium carriers, recombination may be ignored during excitation. Therefore the experimentally determined relative change in photoconductivity, $\Delta\sigma/\sigma$, is equal to $\Delta n/n$ where n is the free carrier concentration. In Fig. 2 it is seen that the probability of photoexcitation $W_i/W_d = \sigma_i/\sigma_d$ depends on the electric field as $\propto \exp(E^2/E_c^2)$. The magnitude of the characteristic field E_c does not depend on the wavelength in the present spectral range between 90.5 and 250 μm, but it is significantly lower for lower temperatures. As has been shown in [10] this observation rules out other mechanisms of nonlinear optical excess carrier generation like multiphoton transitions [17,18], light impact ionization [19], and photon-assisted tunneling [20], which all show a characteristic wavelength dependence.

The fact that the photoconductivity is independent of the wavelength, the exponential dependence of σ_i/σ_d on the square of the electric field of the radiation, and the variation of the signal with temperature permit one to conclude that free carriers are generated by phonon-assisted tunnel ionization of DX^- centers with far-infrared radiation. As is seen from Fig. 2, at high field strengths the ionization probability increases more slowly than $\exp(E^2/E_c^2)$ with increasing electric field E. Such behavior may be attributed to a transition of the ionization process from phonon-assisted tunneling to direct tunneling in agreement with theoretical [8,9] and experimental results [21].

The tunneling time τ_2 is calculated as a function of temperature from the experimentally determined square of the characteristic field, $E_c^2 = (3m^*\hbar)/(e^2\tau_2^3)$, which is taken from Eq. (1). In Fig. 3 τ_2 of the DX^- center in $Al_xGa_{1-x}Sb$, $x = 0.5$ is plotted versus the reciprocal temperature $1/T$. For the purpose of comparison Fig. 3 also contains an $\hbar/2k_BT$ curve and the tunneling time τ_2 of

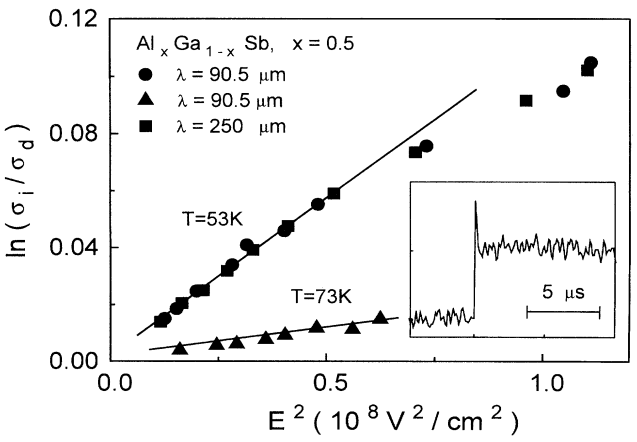

FIG. 2. Dependence of $\ln(\sigma_i/\sigma_d)$ for DX^- centers in $Al_xGa_{1-x}Sb$, $x = 0.5$, on the square of the amplitude of the electric field of the radiation at different temperatures and wavelengths. The inset shows the oscillogram of the photoconductivity response of $Al_xGa_{1-x}Sb$, $x = 0.5$ at $T = 77$ K on a single laser pulse of $\lambda = 90.5$ μm.

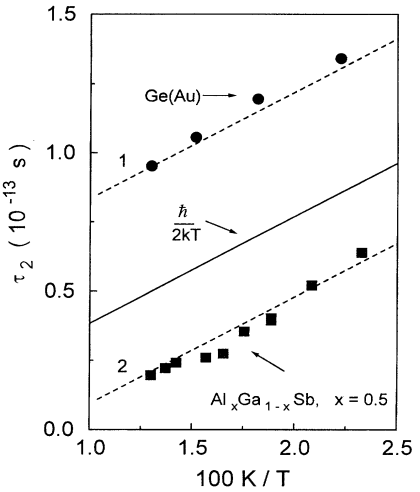

FIG. 3. Tunneling time τ_2 calculated from the experimental characteristic fields E_c as a function of inverse temperature. Squares: DX^- centers in $Al_xGa_{1-x}Sb$, $x = 0.5$; circles: Ge(Au). Broken lines 1 and 2 show fits after $\tau_2 = \hbar/2kT \pm \tau_1$ with $\tau_1 = 4.5 \times 10^{-14}$ s and $\tau_1 = 2.9 \times 10^{-14}$ s, respectively.

the on-site deep acceptors gold in germanium [binding energy 150 meV, configuration Fig. 1(b)], which we measured by the same method. In both cases τ_2 is of the order of $\hbar/2k_BT$ and follows the $1/T$ temperature dependence. The representation of Fig. 3 unambiguously demonstrates that τ_2 is larger than $\hbar/2k_BT$ for an on-site impurity; however, it is smaller than $\hbar/2k_BT$ for the DX^- centers.

This result clearly proves that the autolocalized and on-site impurities may be distinguished by the tunneling time being determined from phonon assisted tunneling in terahertz fields. Even small changes in τ_2 may be resolved because the emission probability depends exponentially on the third power of the tunneling time. The tunneling time reflects the structure of the potential barriers which are systematically distinct for both potential configurations discussed here.

Financial support by the Deutsche Forschungsgemeinschaft is gratefully acknowledged. S. D. G. thanks A. Ya. Shulman for helpful discussions.

*Permanent address: A.F. Ioffe Physicotechnical Institute, Russian Academy of the Sciences, St. Petersburg, 194021, Russia.

[1] G. M. Martin and S. Makram-Ebeid, in *Deep Centers in Semiconductors,* edited by S. T. Pantelides (Gordon and Breach Science Publisher, New York, 1986).
[2] P. M. Mooney, J. Appl. Phys. **67**, R1 (1990).
[3] P. M. Mooney and T. N. Theis, Comments Condens. Matter Phys. **16**, 167 (1992).
[4] R. C. Newman, Semicond. Sci. Technol. **9**, 1749 (1994).
[5] D. V. Lang and R. A. Logan, Phys. Rev. Lett. **39**, 635 (1977).
[6] D. V. Lang, R. A. Logan, and M. Jaros, Phys. Rev. B **19**, 1015 (1979).
[7] C. H. Henry and D. V. Lang, Phys. Rev. B **15**, 989 (1977).
[8] V. Karpus and V. I. Perel, Zh. Eksp. Teor. Fiz. **91**, 2319 (1986) [Sov. Phys. JETP **64**, 1376 (1986)].
[9] V. N. Abakumov, V. I. Perel, and I. N. Yassievich, *Nonradiative Recombination in Semiconductors,* edited by V. M. Agranovich and A. A. Maradudin, Modern Problems in Condensed Matter Sciences Vol. 33 (North-Holland, Amsterdam, 1991).
[10] S. D. Ganichev, W. Prettl, and P. G. Huggard, Phys. Rev. Lett. **71**, 3882 (1993).
[11] R. Landauer and Th. Martin, Rev. Mod. Phys. **66**, 217 (1994).
[12] L. D. Landau and E. M. Livshitz, *Quantum Mechanics* (Pergamon, Oxford, 1977), p. 185.
[13] B. K. Meyer, G. Bischopink, K. W. Benz, A. Schoener, and G. Pensl, J. Cryst. Growth **128**, 475 (1993).
[14] R. Krause-Rehberg, Th. Drost, A. Polity, G. Roos, G. Pensl, D. Volm, B. K. Meyer, G. Bischopink, and K. W. Benz, Phys. Rev. B **48**, 11 723 (1993).
[15] G. Bischopink, Dissertation, Universität Freiburg, Freiburg, 1992.
[16] W. Rühle, W. Jakowetz, and M. Pilkuhn, in *Luminescence of Crystals, Molecules, and Solutions,* edited by F. Williams (Plenum Press, New York, 1973), p. 444.
[17] L. V. Keldysh, Zh. Eksp. Teor. Fiz. **47**, 1945 (1964) [Sov. Phys. JETP **20**, 1307 (1965)].
[18] W. Böhm, E. Ettlinger, and W. Prettl, Phys. Rev. Lett. **47**, 1198 (1981).
[19] S. D. Ganichev, S. A. Emel'yanov, A. P. Dmitriev, Ya. V. Terent'ev, I. D. Yaroshetskii, and I. N. Yassievich, Zh. Eksp. Teor. Fiz. **90**, 445 (1986) [Sov. Phys. JETP **63**, 256 (1986)].
[20] P. S. S. Guimaraes, B. J. Keay, J. P. Kaminski, S. J. Allen, P. F. Hopkins, A. C. Gossard, L. T. Florez, and J. P. Harbinson, Phys. Rev. Lett. **70**, 3792 (1993).
[21] S. D. Ganichev, J. Diener, and W. Prettl, Solid State Commun. **92**, 883 (1994).